A novel multi-jet burner for hot flue gases of wide range of temperatures and compositions for optical diagnostics of solid fuels gasification/combustion

Weng, Wubin; Borggren, Jesper; Li, Bo; Aldén, Marcus; Li, Zhongshan

Published in:
Review of Scientific Instruments

DOI:
10.1063/1.4979638

2017

Document Version:
Peer reviewed version (aka post-print)

Title paper

A novel multi-jet burner for hot flue gases of wide range of temperatures and compositions for optical diagnostics of solid fuels gasification/combustion

Wubin Weng[1], Jesper Borggren[1], Bo Li[2], Marcus Aldén[1] and Zhongshan Li[1*]

[1]*Division of Combustion Physics, Lund University, P.O. Box 118, S221 00 Lund, Sweden*

[2]*Tianjin University, State Key Laboratory of Engines, No. 92 Weijin Road, Nankai District, Tianjin 300072, China*

**corresponding author's email: Zhongshan.li@forbrf.lth.se*

This is the peer reviewed version of the following article: [W.B. Weng, J. Borgren, B Li, M. Aldén and Z.S. Li, '*A novel multi-jet burner for hot flue gases of wide range of temperatures and compositions for optical diagnostics of solid fuels gasification/combustion*', **Rev. Sci. Instr.** 88, 045104 **(2017)**.], which has been published in final form at: https://doi.org/10.1063/1.4979638.

A novel multi-jet burner for hot flue gases of wide range of temperatures and compositions for optical diagnostics of solid fuels gasification/combustion

Wubin Weng[1], Jesper Borggren[1], Bo Li[2], Marcus Aldén[1] and Zhongshan Li[1*]

[1]*Division of Combustion Physics, Lund University, P.O. Box 118, S221 00 Lund, Sweden*

[2]*Tianjin University, State Key Laboratory of Engines, No. 92 Weijin Road, Nankai District, Tianjin 300072, China*

**corresponding author's email: Zhongshan.li@forbrf.lth.se*

A novel multi-jet burner was built to provide one-dimensional laminar flat flames with a wide range of variable parameters for multipurpose quantitative optical measurements. The burner is characterized by two independent plenum chambers, one supporting a matrix of 181 laminar jet flames and the other supporting a co-flow from a perforated plate with small holes evenly distributed among the jets. A uniform rectangular burned gas region of 70 mm × 40 mm can be generated, with a wide range of temperatures and equivalence ratios by controlling independently the gas supplies to the two plenum chambers. The temperature of the hot gas can be adjusted from 1000 K to 2000 K with different flame conditions. The burner is designed to seed additives in gas or liquid phase to study homogeneous reactions. The large uniform region can be used to burn solid fuels and study heterogeneous reactions. The temperature was measured using two-line atomic fluorescence (TLAF) thermometry and the temperature profile at a given height above the burner was found to be flat. Different types of optical diagnostic techniques, such as line of sight absorption or laser-induced fluorescence, can be easily applied in the burner, and as examples, two typical measurements concerning biomass combustion are demonstrated.

I. INTRODUCTION:

The combustion and gasification of solid fuels, such as biomass, are among the main approaches for energy production in today's society. The combustion of these fuels is related to adverse effects on the climate and the human health due to emission of pollutants[1, 2]. To reduce pollutant emissions and improve the efficiency of the combustion process, understanding the relevant complex processes and related flue gas reactions is necessary. A large amount of

experimental researches were performed on this topic in laboratory-scale furnaces, such as entrained-flow gasifiers/combustors[3-5], drop-tube furnaces[6-9] and single-particle reactors[4, 10, 11] to get some essential information of burning solid fuels, such as mass loss rate, ignition time and flue gas composition. Despite this, parameters such as flame temperature, velocity fields, and species concentrations were needed for a better understanding of the combustion process, where optical measurement techniques are needed. Using optical techniques, especially laser diagnostic techniques, non-intrusive and in-situ measurements of these parameters can be achieved with high spatial and temporal resolution[12]. However, optical techniques can't be applied into these furnaces easily without suitable optical access. Experiments conducted in well-controlled, optically accessible environments are required for accurate analysis. For such studies, a burner with the following criteria can be employed[13]: firstly, laminar flames should be easy to stabilize on the burner, and their hot flue gas above the reaction zone should be homogenous and stable across the burner; secondly, different optical diagnostic techniques, such as line-of-sight techniques, point measurement techniques and planar imaging techniques, should be easily applied; thirdly, flames with a wide range of stoichiometry and temperature should be possible, to provide ample choice of hot gas environment for different type of gasification/combustion and flue gas reactions; lastly, gas and liquid additives should easily be seeded homogeneously as tracers into the reaction environment. For example, a fog of indium chloride water solution should, without clogging, be seeded into the reactant gas mixture, for two-line atomic fluorescence thermometry[14].

Several types of burners aimed to fulfill some of the criteria and functions listed above are summarized here. Many burners have been built for the investigation of some specific combustion characteristics or as calibration source for different laser diagnostic techniques. One

example of such a burner is the water-cooled porous plug burner. In 1954, Spalding and Botha[15] introduced this concept for flame speed measurements. It can provide premixed flat flames on a cooled, porous plate, over a wide range of mixture ratios. Later, the commercially available McKenna Burner[16] was developed. Flat flames with various equivalence ratios and flow rates can be stabilized on the sintered porous disk. However, a large amount of heat from the flat flame is released to the water-cooled burner disk. Moreover, atomic tracer species can hardly be seeded into the reactant gas mixture since the sintered plug of the burner can easily be clogged and contaminated by small salt crystals[13]. Replacing the sintered plug by a perforated flat plate or a honeycomb structure can solve part of this seeding problem. The Meker burner[17] is an example of this type and it consists of a plate with a large number of small circular holes with diameter of 0.9 mm. Similarly, a premixed burner with stainless steel tube was developed by Padley[18]. Recently, the Heat flux burner[19] and the flat flame burner from Hartung[13] are examples of two typical premixed laminar flame burners. Both of them have a perforated burner plate with a hexagonal pattern of small holes with diameter of 0.5 mm. With this design, metal atoms can be introduced into flames. Moreover, a steel honeycomb matrix was used in the burners from Snelling[20] and Hsu[21]. Hsu et al. used this type of burner to provide hot gas environment for the burning of wood pellets and the release of alkali elements was investigated through laser-induced breakdown spectroscopy (LIBS)[21]. However, these burners can only provide hot gas environment in limited flat flame cases. Besides the premixed flat flame, non-premixed or partially premixed flames have also been used to provide a hot gas environment. Struckmeiter[22] developed a partially premixed low temperature burner. In this burner, fuel and oxidizer streams are led through two separate chambers. The burner can provide near-one-dimensional flames accessible to quantitative measurements of molecular species and temperatures below 1500K. The Hencken

burner is a commercially available non-premixed burner. Similar to the burner from Struckmeiter, it also has a rapid mixing of fuel and oxidizer above its surface[23, 24]. Due to the uncooled burner holder, the flame temperature increases gradually with time as the burner heats up. Another non-premixed flat flame burner was designed by Van Eyk[25] to provide a well-defined environment with suitable temperature and good optical access. In this burner fuel was fed through 1 mm diameter stainless steel hypodermic tubes, and a small blue flame cone was produced in the first 5 mm above each fuel port. However, the burner was observed to produce a large outer flame which indicates that only part of the fuel is burned in those small flame cones, even for cases where the overall equivalence ratio is fuel lean. This burner has been used in the study of the release of atomic sodium during the burning of coal particles using planar laser-induced fluorescence (PLIF)[25].

In the present work, a burner producing one-dimensional flat flames was developed, which can provide different hot gas environments with a wide range of temperature (1000 K - 2000 K) and gas composition to imitate the real combustion environment in industry furnaces. Lifted premixed flames are adopted to reduce the heat loss to the burner holder and consequently avoid the contamination by metal materials of the burner. Line-of-sight techniques, point measurement techniques, and 2D imaging techniques can be readily applied on this burner. Different tracers can easily be seeded into the gas mixture. With these features, this burner can be widely adopted in the research of solid fuel gasification/combustion and related flue gas reactions with various advanced laser diagnostic techniques.

II. BURNER DESIGN

The structure of the burner is shown in Fig. 1. The burner is made of stainless steel and is divided into two chambers, a jet-flow chamber and a co-flow chamber, by a divider (7). The jet

flow is introduced into the jet-flow chamber through four inlets (9). With two porous barriers (8) and a convergent flow tube, a uniform laminar flow is obtained and evenly disperses into 181 jet tubes (2). These jet tubes have an inner diameter of 1.6 mm and an outer diameter of 3 mm. Their length of 183 mm ensures the laminar flow in them is fully developed. All the laminar flames are stabilized on these jets. In the co-flow chamber, a uniform laminar co-flow is obtained with two porous barriers (5) and mixed evenly with the jet flow after passing a perforated mask (3). Each jet is surrounded by six small holes in the mask as shown in Figure 1(b). The size of the burner outlet is 60 mm×100 mm. The large rectangular area is suitable for the utilization of different laser diagnostics techniques, such as line-of-sight techniques.

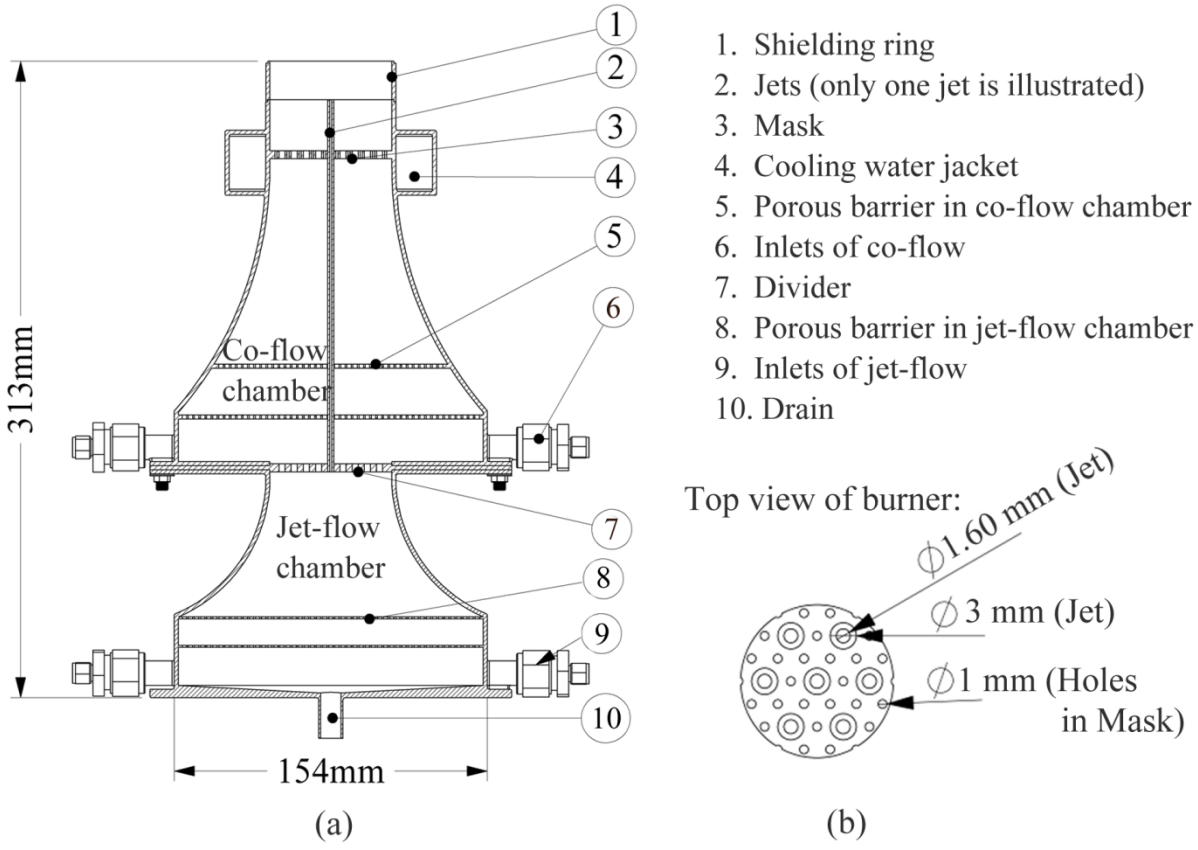

FIG. 1. The structure of the new burner. (a) Sectional view of the burner. (b) Partial top view of the burner.

A cooling water jacket (4) outside the co-flow chamber is installed to cool the burner. On the top of the burner, shielding rings (1) are used to ensure sufficient mixing between co-flow gas and burnt gas from the jet flames and shield the hot gas mixture from the ambient air. The height of each shielding ring is 18 mm. They can be stacked to obtain different measurement positions, i.e. 18 mm, 36 mm, 54 mm and etc., providing different residence time of homogenous reactions. Usually, a rectangular stabilizer is suspended 35 mm above the burner outlet to make the laminar flow more stable. Different tracers can easily be seeded into the gas mixture through either the jet flow or the co-flow. In the jet flow chamber, a drain (10) was incorporated, to remove excess condensate when fog of liquid fuel or water solution is used as seeding tracers.

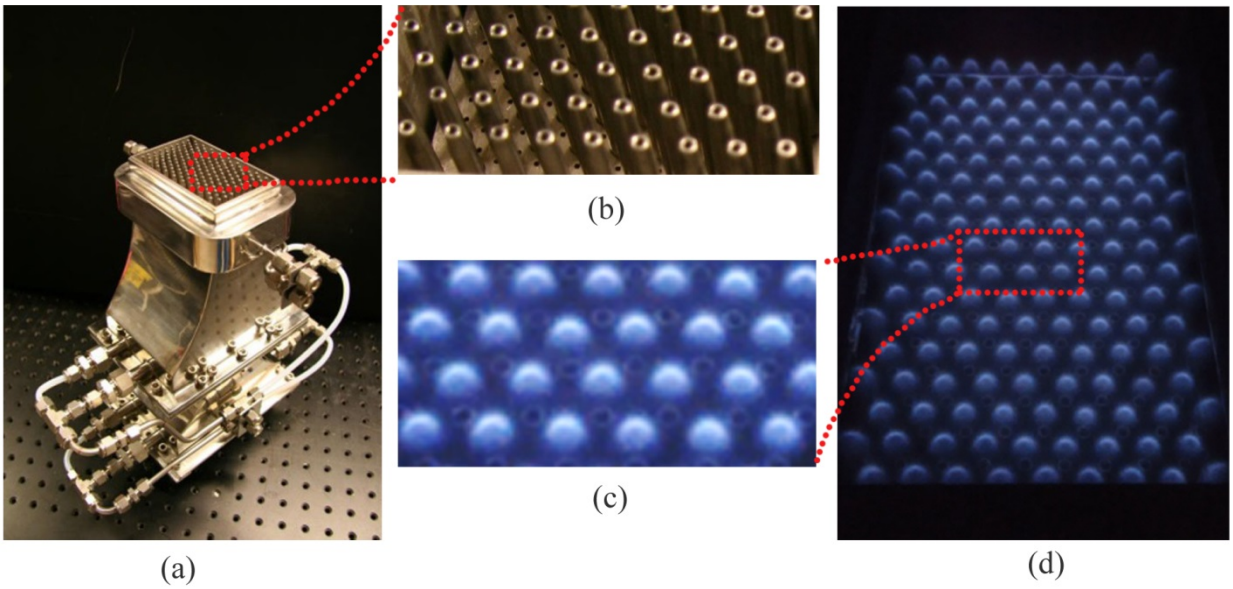

FIG. 2. Photos of the burner (a) and the detail structure of the outlet (b). The photos of typical lifted premixed flame (c) (d).

By varying the gas composition of the jet-flow and the co-flow, either premixed flames or diffusion flames can be generated, and the temperature and composition of the hot flue gas can be controlled. The temperature can be varied in the range of 1000-2000 K. In this work, all gas supplies were controlled by mass flow controllers (Bronkhorst High-Tech) with an accuracy of ±0.8% of the reading value plus ±0.2% of the full scale value.

III. TEMPERATURE CALIBRATION:

A. Flame conditions

TABLE I. Gas flow rate of premixed flame cases.

Case	Equivalence ratio (Φ)	Jet-flow (l/min)			Co-flow (l/min)
		CH_4	O_2	N_2	N_2
PF1	0.6	1.56	5.21	13.46	9.90
PF2	0.7	1.80	5.15	13.30	9.90
PF3	0.8	2.04	5.08	13.13	9.90
PF4	0.9	2.26	5.02	12.97	9.90
PF5	1.0	2.48	4.95	12.54	9.90
PF6	1.1	2.68	4.88	12.39	9.90
PF7	1.2	2.89	4.83	12.24	9.90
PF8	1.3	3.10	4.77	12.09	9.90

TABLE II. Gas flow rate of diffusion flame cases.

Case	Global equivalence ratio (GER)	Jet-flow (l/min)		Co-flow (l/min)	
		CH_4	H_2	O_2	N_2
DF1	0.23	0.79	0.79	8.80	22.89
DF2	0.34	1.19	1.19	8.80	22.89
DF3	0.45	1.58	1.58	8.80	22.89
DF4	0.56	1.98	1.98	8.80	22.89
DF5	0.68	2.38	2.38	8.80	22.89

Temperature is one of the most important parameters for different chemical reactions. Hence, this burner was designed to provide hot flue gas over a wide range of temperature through different flame conditions. Both premixed and diffusion flames can be adopted to provide hot flue gases. For the premixed flames, fuel was introduced into the jet chamber together with the oxidizer. For the diffusion flames, fuel was introduced into the jet chamber, while the oxidizer was delivered through the co-flow chamber. As a calibration, the temperatures of several typical hot gas environments were measured. TABLE I shows different conditions (PF1-PF8) of the premixed flames with equivalence ratio varying from 0.6 to 1.3. TABLE II presents the conditions of the diffusion flames with global equivalence ratio varying from 0.23 to 0.68 (DF1-DF5). In the present measurement, two shielding rings were added to the burner.

Insulation plates (asbestos) with thickness of ~3 mm were put inside the shielding ring to reduce the heat loss. Consequently, the area of the burner outlet was reduced to ~94 mm×54 mm.

B. Laser systems

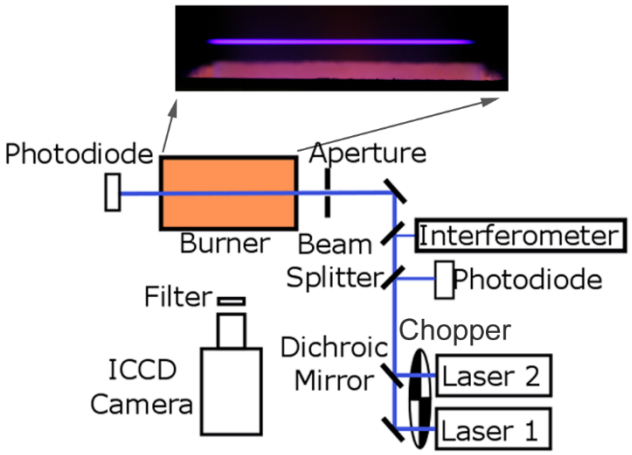

FIG. 3. Schematic setup for the TLAF and a photo of the burner with fluorescence of indium atom shown on the top.

The temperature of the hot flue gas provided by the flames PF1-PF8 was measured using two-line atomic fluorescence (TLAF) thermometry. In the TLAF two different lower levels of the indium atom are excited to a common upper level. The ratio of the fluorescence signals induced by the two excitations is used to derive the temperature[26]. In the present work, a similar measurement system was adopted as the one developed by Borggren et al. with atomic indium[26]. The optical setup is presented in Fig. 3. Two external cavity diode lasers (Toptica, DL100pro and DL100) were employed to provide two continuous-wave lasers with wavelength of 410 and 451 nm to probe the two indium transitions $5^2P_{1/2}\rightarrow6^2S_{1/2}$ and $5^2P_{3/2}\rightarrow6^2S_{1/2}$ respectively. The power of the lasers was about 5 mW. The two lasers were overlapped using a dichroic mirror. A chopper was used to have these two lasers alternatingly. The wavelength and the power were monitored by a wavemeter and a photodiode, respectively. Atomic indium was provided from trimethylindium (TMI) which was seeded into the jet-flow chamber and was burned in the jet flames as described in previous work[27]. The fluorescence of atomic indium was captured by an ICCD camera (Princeton Instrument) and was used to derive temperature.

C. Hot flue gas temperature

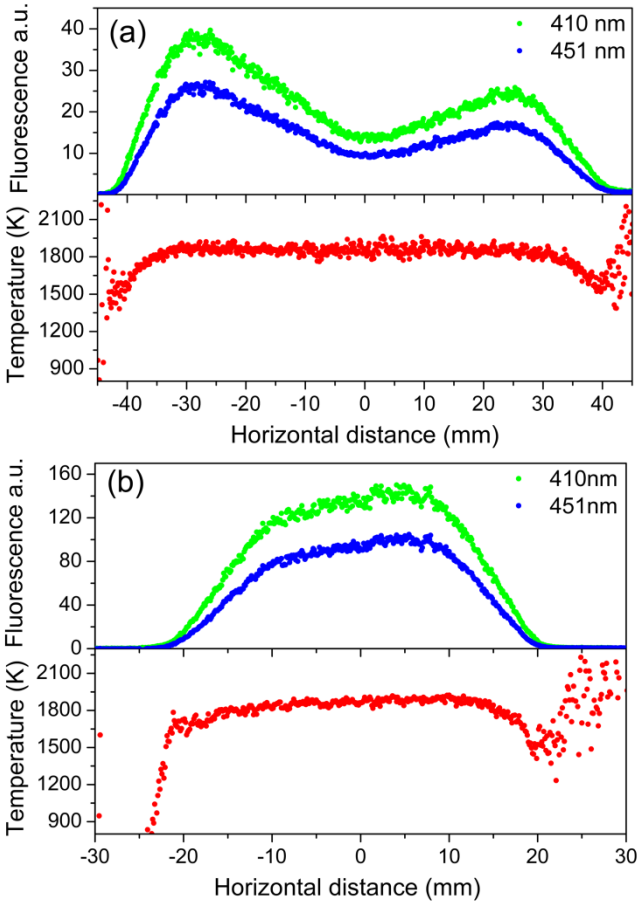

FIG. 4. The distribution of the fluorescence of indium atoms and temperature of the hot flue gas from the flame PF4 along the long side (a) and the short side (b) of the burner.

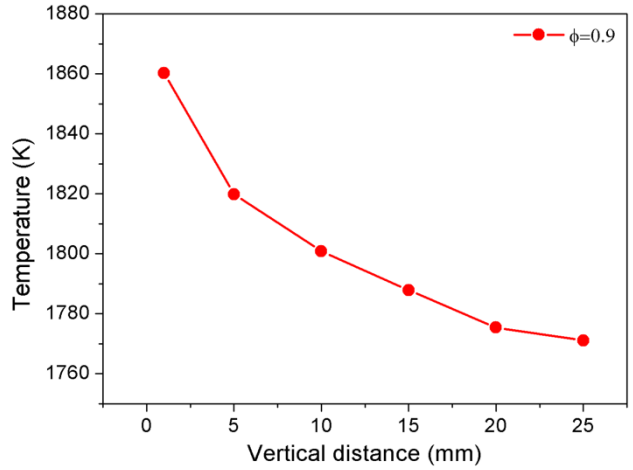

FIG. 5. The temperature measured at different heights above the upper rim of the uppermost shielding ring on the burner with the flame PF4.

The one-dimensional distribution of the fluorescence signal from the excited atomic indium and the temperature derived are presented in Fig. 4. In this case, flame PF4 was adopted and the

measurement height was ~2 mm above the burner outlet. The uneven distribution of the fluorescence signal is most likely the result of TMI sticking on the walls of the burner chamber during its seeding. The release of the indium from the contaminated surface can have a big influence on the distribution of indium atom since the concentration of the indium atom seeded into the flame was very low (< 1 ppm) during the temperature measurement[27]. Nevertheless, the uneven distribution of indium atom does not affect the temperature measurement and the result in Fig. 4 shows that the burner has good spatial uniformity, and the homogeneous area of the temperature field at this height is estimated to be larger than 70 mm×40 mm. Moreover, it is suitable for quantitative measurement and calibration of line-of-sight techniques due to its rectangular shape. The vertical temperature distribution was also measured for flame PF4. As shown is Fig. 5, the temperature has a reduction of ~ 90 K as the vertical position increases from 2 mm to 25 mm. This temperature reduction is mainly caused by the thermal radiation of hot gas to the environment.

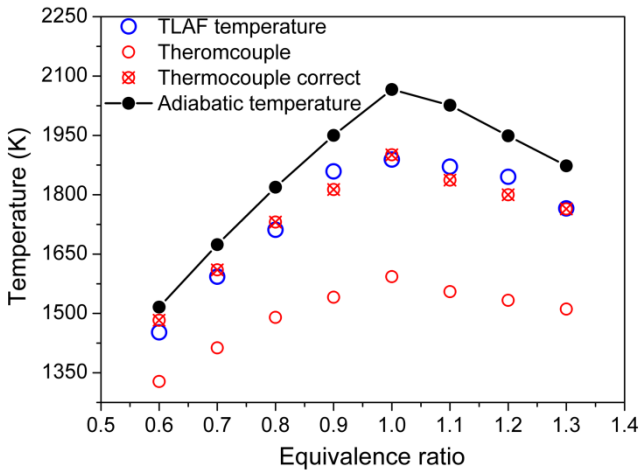

FIG. 6. Temperature of the hot flue gas from the premixed flames (PF1-8) with equivalence ratios from 0.6 to 1.3 measured using different techniques, i.e. TLAF and thermocouple. The measurement position is 2 mm above the burner outlet. Black dots: simulation results; blue circles: results from TLAF measurement; red circles: results from thermocouple measurement.

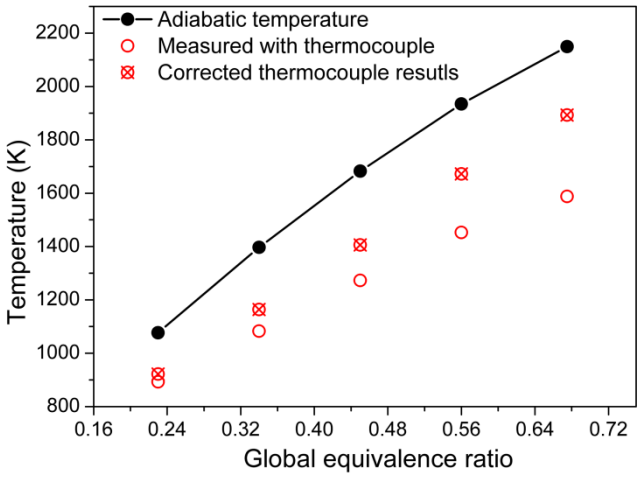

FIG. 7. Temperature of the hot flue gas from the diffusion flames (DF1-5) with different global equivalence ratio from 0.23 to 0.68. measured using a B type thermocouple. The measurement position is 2 mm above the burner outlet. Black dots: simulation results; red circles: results from thermocouple measurement.

Fig. 6 presents the temperature of the hot flue gas from different premixed flames. Simulation results were obtained through the chemical equilibrium model in Chemkin[28] using GRI-mech 3.0[29], which predicts a similar trend as the experiments. The measured temperature values are lower since the flames in our experiments are not perfectly adiabatic. The biggest deviation appears near the stoichiometric condition, because the highest laminar flame speed achieved at this condition brings the flame closest to the jet tubes and hence, causes the largest heat loss to the burner.

The temperature was also measured by a B type thermocouple with a wire diameter of 0.25 mm. The temperature measured by the thermocouple is much lower than that by the TLAF thermometry. This deviation is caused by the heat loss through the thermal radiation in the hot thermocouple conjunction with its size around 1 mm to the cool ambient environment and the burner below the flame. Hence, the thermocouple base temperature was corrected based on heat transfer theory[30, 31]. Since the shape of the thermocouple conjunction is not perfectly spherical, its diameter used in the correction was estimated to 1.12 mm to have the minimized deviation between the corrected results and the results from TLAF measurements. The corrected results

were shown is Fig. 6 with the correction process in supplementary material.

In addition to the premix laminar flames, the temperature of several diffusion flames, from DF1 to DF5, were also measured. Diffusion flames are more stable, and their temperatures are easier to vary. However, compared with lifted premixed flames, they suffer much larger heat loss because they almost anchored on the jet tubes, and need much more oxygen to avoid soot generation. For the diffusion flames, the temperature measurements were only performed with the thermocouple because the TLAF thermometry becomes unavailable when the hot gas contains a high percentage of oxygen, and oxidation of atomic indium reduces the fluorescence signal significantly. As shown in Fig. 7, for diffusion flames, the temperature can be varied from 1000 K to 1800 K. After correction, the measured result was about 200 K lower than the simulations. The difference was much larger compared with the lifted premixed flame (~100 K), because of the larger heat loss in the diffusion flames.

IV. APPLICATION IN HETEROGENEOUS CHEMICAL REACTION

This novel burner setup is suitable for applying optical techniques to solid fuel combustion/gasification researches. The hot flue gases can provide a wide range of temperatures and gas compositions that can be used to imitate the real combustion environment in industry furnaces.

Table III. Flame cases for temperature and oxygen concentration varying.

Case	Equivalence ratio (Φ)	Jet-flow (l/min)			Co-flow (l/min)		O_2 in flue gas (%)	Temperature of flue gas (K)
		CH_4	O_2	N_2	N_2	O_2		
O1	0.8	2.04	5.08	13.13	9.90	0.00	3.30	1747
O2	0.8	2.04	5.08	13.13	7.81	2.09	10.10	1731
T1	0.6	1.56	5.21	13.46	9.90	0.00	6.81	1486
T2	1.2	2.89	4.83	12.52	6.88	3.03	6.74	1964

As an example, the time-resolved emission spectrum of burning straw pellets in different hot gas environments was measured. The straw pellets were cylindrical, 8 mm in diameter and 5 mm in height. The mass of a single pellet was 45±5 mg. The pellet was held by two thin ceramic rods with a diameter of 0.8 mm and was placed at the height of 1 mm above the burner outlet. The ceramic rods were fixed on a sensitive scale to record the mass loss process of the burning pellets. Four flame cases were used to provide specific hot gas environments, as shown in TABLE III. In cases O1 and O2, the oxygen concentration was either 3.3% or 10.1% with the temperature at ~1740 K. In cases T1 and T2, the temperature was 1486 K and 1964 K with fixed oxygen concentration around 6.8%.

The burning of the pellets was stable and was isolated from the ambient environment thanks to the large volume of the hot flue gas. The photos in Fig. 8 are the burning pellets in the de-volatilization stage taken at ~50 seconds after the burning begins. The bright light of the plume above the burning pellets mainly comes from Plank radiation of soot and atomic emission of sodium. The emission becomes stronger when the gas environment contains more oxygen or has a higher temperature. To get the emission spectrum, a spectrometer (USB 2000+, Ocean Optics) with a spherical lens (f = +100 mm) was employed. The focus of the spectral collection volume was in the middle of the plume and at 2 mm above the surface of the pellet. The emission spectrum from 400 nm to 850 nm is shown in Fig. 8. Similar to the phenomenon from those photos, the intensity of the spectrum became stronger with higher oxygen concentration or temperature. Emission of atomic sodium (589.0 nm / 589.6 nm) and atomic potassium (766.5 nm / 769.9 nm) was observed, which indicates that some sodium and potassium species were released during the burning of straw pellets.

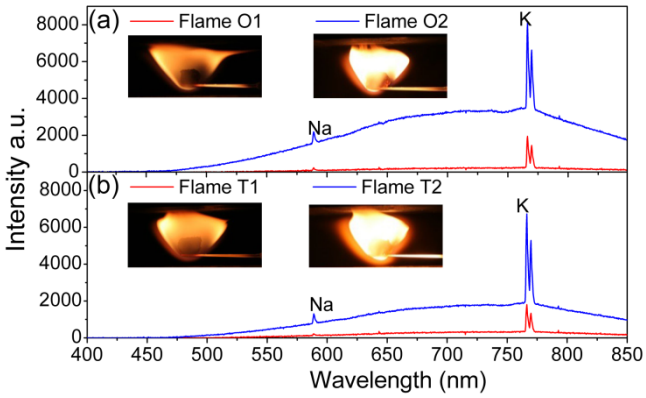

FIG. 8. The emission spectrum of the burning straw pellets recorded at ~50 seconds in the hot gas environment with different oxygen concentration (a) and the hot gas environment with different temperature (b). The photos of burning pellets in Flame O1 ((a) left) and Flame O2 ((a) right); the photos of burning pellets in Flame T1 ((b) left) and Flame T2 ((b) right). Note: the spectrometer can have different sensitivity to the signal at different wavelength.

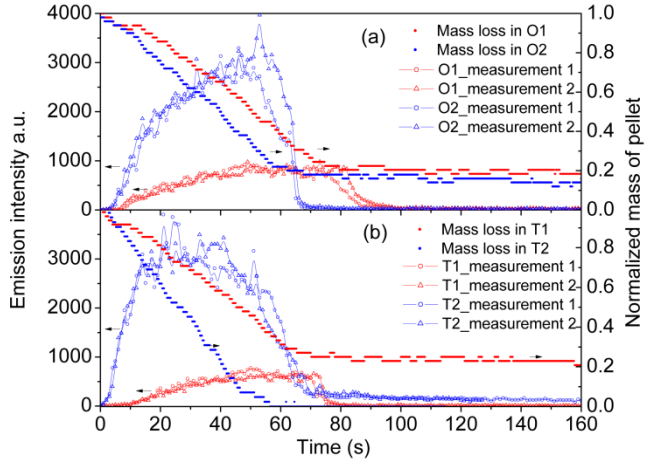

FIG. 9. Temporally resolved emission intensity of atomic potassium and mass-loss of the burning pellets in the hot gas environment with different oxygen concentration (a) and the hot gas environment with different temperature (b).

Figure 9 shows the variation of the emission strength of atomic potassium in the burning period of the first 160 seconds with the corresponding variation of mass loss. The emission of atomic potassium shows a strong relationship with the mass loss. The moment when the atomic emission and the mass become constant is considered as the end of the de-volatilization stage. Higher temperature results in larger mass loss rate and stronger emission intensity, as shown in Fig. 9 (b). With higher oxygen concentration, the burning of the volatile gas became more intense, which formed higher temperature environment for the burning pellets, and hence, the concentration of oxygen has similar effect as the temperature of the hot flue gas.

This test indicates that the burner can provide various hot gas environments and it is convenient to apply optical techniques to the study of heterogeneous reactions, such as biomass combustion/gasification. To have more information about the release of potassium, several other methods can be employed, such as laser-induced breakdown spectroscopy (LIBS)[21], laser-induced photo-fragment[32], and absorption spectroscopy[33].

V. APPLICATION IN HOMOGENEOUS CHEMICAL REACTION

This burner is also a powerful tool in the research of homogenous chemical reactions. Different tracers can be easily seeded into the flame, and can be used to investigate flue gas reactions, e.g. reactions in alkali species controlling using sulfur species or NO_x emission reduction through NH_3 seeding.

As an example, the absorption spectra of gas phase potassium chloride (KCl) and potassium hydroxide (KOH) in the hot flue gases were measured. According to the results of section IV, some potassium is released during the burning of biomass fuels, which mainly exists in the form of potassium chloride (KCl) and potassium hydroxide (KOH) according to previous studies[34, 35]. KCl can cause severe problem to a running furnace, through e.g. fouling and corrosion[36].

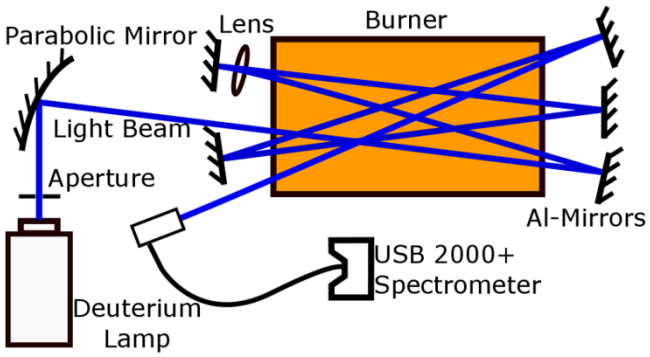

FIG. 10. The optical setup of the UV absorption measurement.

A typical optical setup for UV absorption measurement is shown in Fig. 10. A broadband

UV light was produced by a deuterium lamp and passed above the burner after an aperture and a parabolic mirror. The diameter of the light beam is about 10 mm and one spherical lens (f = +1000 mm) was used to collimate the light beam. Five UV enhanced aluminum mirrors were used to increase the optical absorption length. The total absorption length was about 575 mm. A spectrometer (USB 2000+, Ocean Optics) was employed to collect the transmitted light beam. To produce gas phase KCl/KOH, a water solution of KCl (0.5 mole/l) or KOH (0.5 mole/l) was used. It was introduced into the jet flow chamber in the form of fog which was generated by an ultrasonic fog generator, and it was well-mixed in the jet flow chamber. The fog of salt water solution was atomized after passing through the jet flames. In the hot gas environment, chemical equilibrium condition was achieved forming gas-phase KCl or KOH, considering that the chemical reaction time was much less than 0.01 seconds based on simulation[37], which is shorter than the residence time, about 0.06 seconds, from the flames to the measurement position.

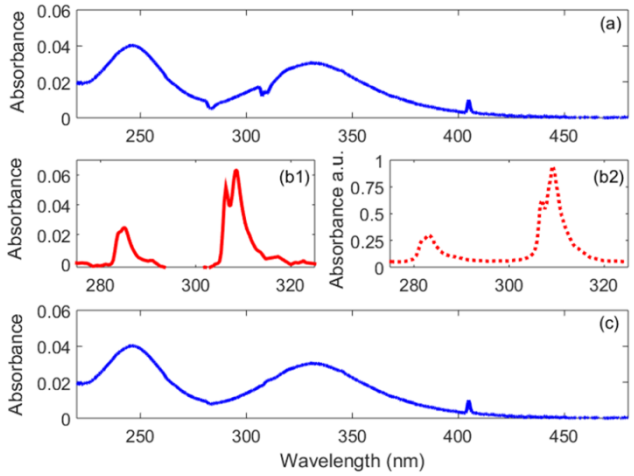

FIG. 11. UV absorption spectra in the flue gas. (a) UV absorption spectrum with KOH seeding; (b1) Absorption spectrum of OH in the flame; (b2) Simulated absorption spectrum of OH using LIFBASE; (c) UV absorption spectrum with KOH seeding after the correction using the OH spectrum.

The measurement was conducted in flame PF4. The temperature of the hot flue gas was about 1850 K. After the KOH solution being seeded, the absorption spectrum (*absorbance=ln(UV spectrum without seeding/UV spectrum with seeding)*) was obtained and is

shown in Fig. 11 (a) in the wavelength range from 220 nm to 480 nm. The two broad peaks at 250 nm and 330 nm, in Fig. 11 (c) are from the gas phase KOH. For the UV absorption spectrum of KOH, the only information which can be referred to is the collinear photo-fragmentation and absorption spectroscopy of KOH at 873 K[32] and the UV absorption spectrum of sodium hydroxide (NaOH) [38]. At 405 nm, the absorption peak of atomic potassium (404.4 nm and 404.7 nm) is observed. Even though the concentration of the atomic potassium is low, its large atomic absorption cross section can still cause a substantial absorption. Moreover, there are OH radicals in the hot gas, causing absorption at wavelengths around 283 nm and 310 nm. In Fig. 11 (b), the measured absorption spectrum of OH in the hot flue gas without seeding ((*absorbance=ln(UV spectrum without flame/UV spectrum with flame but without seeding)*)) was presented together with the simulation one from LIFBASE[39]. They have very similar structure. Hence, the interference on the absorption spectrum in Fig. 11 (a) at wavelength around 283 nm and 310 nm was confirmed from the absorption of hydroxyl (OH) radicals. The dips in the spectrum around these two wavelengths indicate a reduction of OH radicals upon seeding of KOH. Since the temperature change caused by the seeding is small, less than 5 K, this reduction can be caused by the additional reactions such as the enhancement of OH radicals consumption by atomic potassium[18]. Using the measured OH spectrum, the spectrum in Figure 11 (a) was corrected to the pure KOH spectrum as shown in Figure 11 (c).

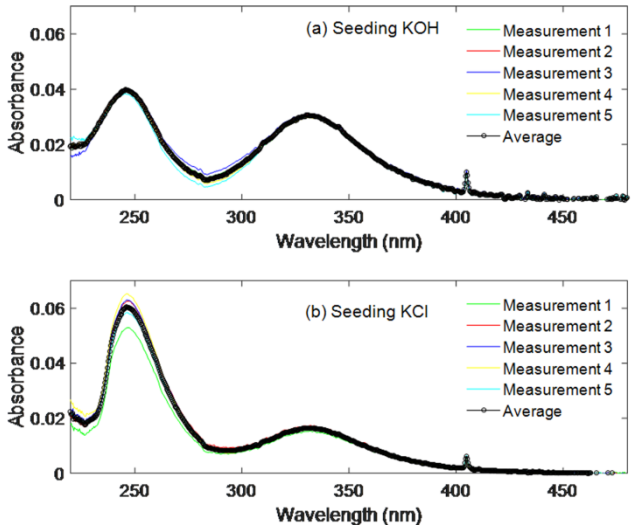

FIG. 12. (a) Absorption spectrum of the flame with KOH seeding (b) Absorption spectrum of the flame with KCl seeding.

Similarly, the UV absorption of the flame with the seeding of KCl solution was obtained and shown in Fig. 12 (b). This spectrum was thought to contain absorbance of both KCl and KOH according to the chemical equilibrium analysis. In the simulation using the equilibrium model in CHEMKIN and the mechanism focusing on the potassium reactions[37, 40], 70% KCl transforms to KOH, as the KCl was seeded into the flue gas with concentration of 100 ppm. These spectra obtained show to have a good signal-to-noise ratio despite the small absorption cross sections of gas phase KCl (0.74×10^{-21} m^2) and KOH (0.5×10^{-21} m^2)[32] due to the large size of the burner outlet.

VI. CONCLUSION

A novel multi-jet burner was developed aiming at the investigation of different high temperature chemical reactions with various advanced optical techniques. The burner can provide hot flue gas flows with a wide range of temperatures and a large measurement region. Various tracers can be seeded into it easily. The temperature of the hot flue gases from different lifted premixed flame with equivalence ratio changing from 0.6 to 1.3 was measured by two-line

atomic fluorescence thermometry. The temperature distribution of the hot flue gas from the burner was obtained and was proved to have an isothermal area of 70 mm × 40 mm.

To test the performance of the burner, two optical measurements at high temperature were conducted. In the first measurement the emission spectrum of a burning straw pellet was measured, which shows that the burner is suitable for optical diagnostic of heterogeneous reactions, with its advantages of large uniform hot gas region isolating the heterogeneous reaction from the influence of the cool ambient environment, the accurately controlled hot gas temperature and composition, and the applicability of various optical techniques. In the second measurement, an UV absorption spectrum of potassium chloride and potassium hydroxide was recorded, and this measurement indicates that this burner can also be utilized in the study of homogenous chemical reactions with its advantages such as tracer seeding and uniform hot gas environment.

SUPPLEMENTARY MATERIAL

See supplementary material for the process correcting raw thermocouple readings based on heat transfer theory.

ACKNOWLEDGEMENTS

The work was financially supported by the Swedish Energy Agency, the Knut & Alice Wallenberg foundation, the Swedish Research Council (VR) and the European Research Council (Advanced Grant TUCLA program). Bo Li would like to thank the financial support from the Natural Science Foundation of China (91541119, 51320105008, 91541203).

REFERENCES

[1]B. M. Jenkins, L. L. Baxter, T. R. Miles Jr and T. R. Miles, Fuel Process. Technol. **54** (1–3), 17 (1998).
[2]A. Williams, J. M. Jones, L. Ma and M. Pourkashanian, Prog. Energy Combust. Sci. **38** (2), 113 (2012).
[3]J. J. Hernández, G. Aranda-Almansa and A. Bula, Fuel Process. Technol. **91** (6), 681 (2010).
[4]L. Hong, Doctoral Dissertation, Brigham Young University Provo, 2006.
[5]J. Zhou, Q. Chen, H. Zhao, X. Cao, Q. Mei, Z. Luo and K. Cen, Biotechnol. Adv. **27** (5), 606 (2009).
[6]R. Khatami, C. Stivers, K. Joshi, Y. A. Levendis and A. F. Sarofim, Combust. Flame **159** (3), 1253 (2012).
[7]Y. A. Levendis, K. Joshi, R. Khatami and A. F. Sarofim, Combust. Flame **158** (3), 452 (2011).
[8]J. Riaza, R. Khatami, Y. A. Levendis, L. Álvarez, M. V. Gil, C. Pevida, F. Rubiera and J. J. Pis, Biomass Bioenergy **64** 162 (2014).
[9]C. Zou, L. Cai, D. Wu, Y. Liu, S. Liu and C. Zheng, Proc. Combust. Inst. **35** (3), 3629 (2015).
[10]F. Shan, Q. Lin, K. Zhou, Y. Wu, W. Fu, P. Zhang, L. Song, C. Shao and B. Yi, Fuel **188** 277 (2017).
[11]O. Karlström, M. Perander, N. DeMartini, A. Brink and M. Hupa, Fuel **190** 274 (2017).
[12]A. C. Eckbreth, *Laser Diagnostics for Combustion Temperature and Species* (Gordon and Breach Publishers, 1996).
[13]G. Hartung, J. Hult and C. F. Kaminski, Meas. Sci. Technol. **17** (9), 2485 (2006).
[14]J. Nygren, J. Engström, J. Walewski, C. F. Kaminski and M. Aldén, Meas. Sci. Technol. **12** (8), 1294 (2001).
[15]J. P. Botha and D. B. Spalding, Proc. R. Soc. London, A **225** (1160), 71 (1954).
[16]S. Prucker, W. Meier and W. Stricker, Rev. Sci. Instrum. **65** (9), 2908 (1994).
[17]W. Snelleman and J. A. Smit, Metro **4** (3), 123 (1968).
[18]P. J. Padley and T. M. Sugden, Proc. R. Soc. London, A **248** (1253), 248 (1958).
[19]K. J. Bosschaart and L. P. H. de Goey, Combust. Flame **132** (1–2), 170 (2003).
[20]D. R. Snelling, G. J. Smallwood, R. A. Sawchuk and T. Parameswaran, Appl. Opt. **26** (1), 99 (1987).
[21]L. J. Hsu, Z. T. Alwahabi, G. J. Nathan, Y. Li, Z. S. Li and M. Aldén, Appl. Spectmsc. **65** (6), 684 (2011).
[22]U. Struckmeier, A. Lucassen, N. Hansen, T. Wada, N. Peters and K. Kohse-Höinghaus, Combust. Flame **157** (10), 1966 (2010).
[23]W. D. Kulatilaka, R. P. Lucht, S. F. Hanna and V. R. Katta, Combust. Flame **137** (4), 523 (2004).
[24]E. R. Furlong, D. S. Baer and R. K. Hanson, Symp. (Int.) Combust. **26** (2), 2851 (1996).
[25]P. J. van Eyk, P. J. Ashman, Z. T. Alwahabi and G. J. Nathan, Combust. Flame **155** (3), 529 (2008).
[26]J. Borggren, I. S. Burns, A.-L. Sahlberg, M. Aldén and Z. Li, Appl. Phys. B **122** (3), 58 (2016).
[27]R. Whiddon, B. Zhou, J. Borggren, M. Aldén and Z. S. Li, Rev. Sci. Instrum. **86** (9), 093107 (2015).
[28] *CHEMKIN 10131, Reaction Design: San Diego, 2013*.
[29]G. Smith, D. Golden, M. Frenklach, N. Moriarty, B. Eiteneer, M. Goldenberg and e. al., *GRI-Mech 3.0. http://www.me.berkeley.edu/gri_mech/*.
[30]http://www.matfys.lth.se/education/FMFF05/Radiation%20correction%20(for%20diskussionen).docx.
[31]D. Bradley and A. G. Entwistle, Br. J. Appl. Phys. **12** (12), 708 (1961).
[32]T. Sorvajärvi, N. DeMartini, J. Rossi and J. Toivonen, Appl. Spectmsc. **68** (2), 179 (2014).
[33]Z. Qu, E. Steinvall, R. Ghorbani and F. M. Schmidt, Anal. Chem. **88** (7), 3754 (2016).
[34]S. C. van Lith, P. A. Jensen, F. J. Frandsen and P. Glarborg, Energy Fuels **22** (3), 1598 (2008).
[35]H. Fatehi, Y. He, Z. Wang, Z. S. Li, X. S. Bai, M. Aldén and K. F. Cen, Proc. Combust. Inst. **35** (2), 2389 (2015).
[36]H. P. Nielsen, F. J. Frandsen, K. Dam-Johansen and L. L. Baxter, Prog. Energy Combust. Sci. **26** (3), 283 (2000).
[37]L. Hindiyarti, F. Frandsen, H. Livbjerg, P. Glarborg and P. Marshall, Fuel **87** (8–9), 1591 (2008).
[38]D. E. Self and J. M. C. Plane, Phys. Chem. Chem. Phys. **4** (1), 16 (2002).
[39] *LIEBASE (version 2.1) https://www.sri.com/contact/form/lifbase*.
[40]B. Li, Z. Sun, Z. Li, M. Aldén, J. G. Jakobsen, S. Hansen and P. Glarborg, Combust. Flame **160** (5), 959 (2013).